Source Time Function of Caspian Basin and Surrounding Area Earthquakes

Mehrdad Mostafazadeh[1] and Mohammad Mokhtari[2]

1. Assistant Professor, International Institute of Earthquake Engineering and Seismology, Tehran, I.R. Iran, e-mail: mehrdad@iiees.ac.ir
2. Assistant Professor, International Institute of Earthquake Engineering and Seismology, Tehran, I.R. Iran, e-mail: mokhtari@iiees.ac.ir

ABSTRACT: *The south Caspian Basin is a seismic block within the Alpine-Himalayan Belt. The source time function of 31 events of Caspian earthquakes have been obtained from teleseismic body waveform modeling. The duration of each subevent with magnitude larger than 5 (M_w>5.0) and depth between $4 \le h \le 76$km was determined from source time function. Corner frequency and stress drops have been calculated for each of 31 events by using pulse duration from source time function.When viewed over the entire depth range, the total duration (τ_t) is related to Mo by $\log \tau_t$ = (0.2642 $\pm$ 0.001) log M_O- 8.9119 ($\pm$.0.194). Corner frequencies range is from 0.038Hz to 0.16Hz. Static stress drops calculated from the pulse shapes for each event studied in this paper changed between 0.07 bars to a maximum of 46 bars. Minimum and maximum displacements are 0.79m and 3.3m respectively. The variation in stress drop is considerable, but no evidence is seen for a scaling relation in which stress drop increase with moment. These relative source durations do not show any clear depth dependence.*

Keywords: Source time function; Caspian sea; Continental plates; Waveform modeling

1. Introduction

Earthquake source time duration is an important characteristic of the rupture process. Whereas shallow earthquakes can be explained by a process involving simple failure or slip on a frictional surface, the mode of stress release at depths where the overburden pressure is too large to allow for simple frictional sliding is still a matter of much debate. Because of its dependence upon important characteristics of the rupture such as fault size, stress drop, and rupture velocity, earthquake duration is a potentially powerful, if somewhat imprecise; discriminate between mechanical models of deep earthquakes.

Body waveform modeling has become one of the most important tools available to seismologist for refining earth structure models and understanding fault-rupturing process. Three component waveform data from the far-field *GDSN* stations in the epicentral range 30°-90° were obtained for the selected earthquakes. *SYN3* algorithm McCaffery and Abers [19] and *IASPEI SYN4* algorithm McCaffery et al [20], which is a recent version of Nabelek [21] inversion procedure based on a weighted least squares method, was used for waveform inversion. The source time function (described by a series of overlapping isosceles triangles), centroid depth, and the fault orientation parameters (strike, dip, and the rake) are used in order to compute synthetic seismograms and the seismic moment by Priestley et al [22] and Jackson et al [15].

In terms of the details of fault rupture or source complexity, our knowledge of the very large earthquakes is limited. Until recently, most of what was known about major earthquakes consisted of estimates of their focal mechanism and moment. Although this information is of fundamental interest, it is desirable to know more about the spatial and

temporal distribution of moment release [11]. The teleseismic source time function gives information about the fault rupture or source complexity. The relationship between the seismic moment, M_O, and source duration, τ_t, provides information on the mechanics of faulting in the earth's interior. In this paper, the results of a survey study of teleseismic source time functions for major shallow earthquakes in south of Caspian Basin and surrounding area studied by Priestley et al [22] and Jackson et al [15] have been used, see Table (1).

Defining the link between the radiated seismic waves of earthquakes and the fault properties is the central problem in earthquake seismology. Brune [2, 3] gave a rather simple set of formulas that allowes the determination of stress drop, source radius, corner frequency and moment from spectra of the body wave. The possibility that there is a relation between the seismic stress drop and shear stress on the fault suggested that a synthesis of stress drop values might yield insight into the level of stress on the fault, spatial and temporal variations in shear stress, and even the stresses that drive the plate motions. There is some suggestion that earthquakes from different tectonic regions have systematically different values of apparent stress or stress drop [26].

The essential purpose of this study is to evaluate fault rupture or source complexity and prepare information about the time history of displacement on the fault. In addition, the evaluation of the seismic moment-duration and any interpretation of any relation between stress drop and depth of earthquakes

Table 1. Earthquake hypocentral data [15, 22].

No	Date d m y	Origin Time	Latitude (N^0)	Longitude (E^0)	Depth (Km)	M_w	M_O(N-m)
1	01 09 1962	19:20	35.63	49.87	10	7.0	3.68E+19
2	03 01 1969	03:16	37.10	57.83	7	5.5	1.89E+17
3	30 07 1970	00:52	37.85	55.94	11	6.3	4.29E+18
4	14 02 1971	16:27	36.62	55.74	11	5.7	4.05E+17
5	04 11 1978	15:22	37.71	48.95	21	6.1	1.90E+18
6	04 05 1980	18:35	38.09	49.07	15	6.3	4.02E+18
7	19 12 1980	01:16	34:50	50.67	14	6.0	1.40E+18
8	22 12 1980	12:51	34.49	50.67	15	5.6	2.81E+17
9	04 08 1981	18:35	38.21	49.41	20	5.6	2.38E+17
10	22 07 1983	02:41	36.98	49.23	10	5.6	1.88E+17
11	22 02 1984	05:44	39.52	54.11	27	5.7	5.10E+17
12	29 10 1985	13:13	36.75	54.81	13	6.2	2.18E+18
13	06 03 1986	00:05	40.37	51.60	35	6.2	2.43E+18
14	07 09 1987	11:32	39.37	54.76	30	5.5	2.33E+17
15	16 09 1989	02:05	40.34	51.53	31	6.5	6.84E+18
16	17 09 1989	00:53	40.20	51.75	35	6.2	2.17E+18
17	21 06 1990	09:02	36.61	49.81	10	5.6	2.91E+17
18	28 11 1991	17:20	36.84	49.61	8	5.7	3.89E+17
19	31 08 1993	06:55	41.87	49.47	76	5.1	6.33E+16
20	01 07 1994	10:12	40.19	53.35	42	5.6	2.93E+17
21	01 07 1994	19:50	40.20	53.37	41	5.1	5.95E+16
22	29 10 1995	06:27	39.56	51.90	61	5.3	1.22E+17
23	04 02 1997	09:53	37.39	57.33	13	5.4	1.61E+17
24	04 02 1997	10:37	37.39	57.35	8	6.4	5.75E+18
25	28 02 1997	12:57	38.10	47.79	9	6.0	1.20E+18
26	09 07 1998	14:19	38.71	48.50	27	5.6	4.38E+17
27	22 08 2000	16:55	38.07	57.19	4	5.6	3.09E+17
28	25 11 2001	18:09	40.29	50.06	40	6.2	2.34E+18
29	25 11 2000	18:10	40.31	50.09	33	6.1	1.67E+18
30	06 12 2000	17:11	39.40	55.04	31	6.9	2.41E+19
31	10 06 2001	01:52	39.83	53.89	31	5.3	1.17E+17

have been carried out, see Table (1). And finally a rupture model map of seismic events that occurred in Caspian and surrounding area have been introduced. Figure (1) shows the distribution of epicenter location of earthquakes that are used in this study.

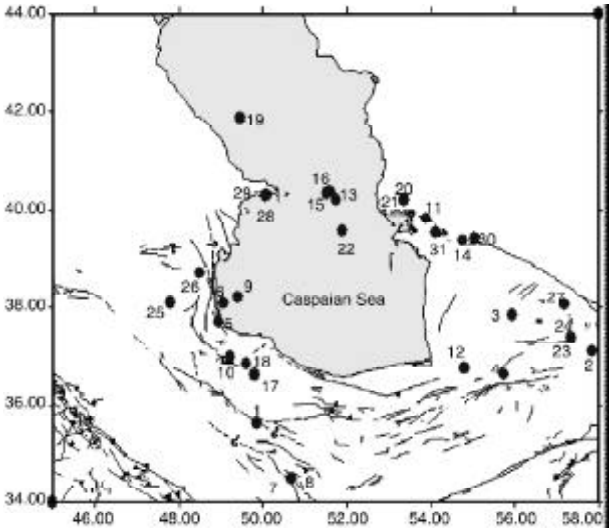

Figure 1. Map showing the distribution of epicenter of earthquakes studied in this paper, see Table (1).

2. Previous Works

Three measures of source duration of an earthquake have been reported in the literature (Figure (2) taken from Singh et al [24]): the total rupture duration (τ_t), the pulse duration of each subevent of a complex earthquake (τ_p), and rise time (τ_r).

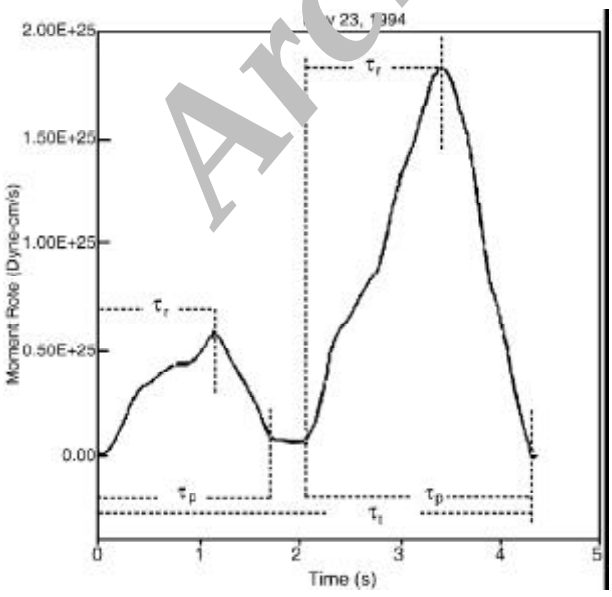

Figure 2. An example of three measures of source duration of an earthquake (taken from Singh et al [24]).

It is well known that a constant stress drop source model implies that Mo/τ^3 is a constant. For shallow earthquakes, the reported values of M_O/τ_t^3 lie between 0.25×10^{23} and 1.0×10^{23} dyne cm/s^3 [7, 8, 9, 18]. These results were obtained from the analysis of teleseismic data. Kikuchi and Ishida [17] studied source time function (*STF*) and subevent pulse duration, τ_p, of earthquakes in the Kanto region of Japan, which were recorded by broadband seismographic network near the epicentral region. Focal depths of Kanto earthquakes that examined had focal depths between 50 and 125*km* [17]. Kikuchi and Ishida [17] reported $M_O/\tau_p^3 \sim 1\times10^{24}$ dyne cm/s^3 for intermediate seismicity. Bos et al [5] studied the source duration and depth of deep (h>300km) earthquakes, and they have observed a slight decrease in duration with depth. They have suggested that the total duration satisfy least square fit of

$$t_{tot} = (9.77\pm0.2\text{c}) + (3.59\pm0.82)\times10^{-3}\ H$$

where earthquake depth H is in kilometers and t is in seconds.

3. Fault Complexity and Age of Lithosphere

The source complexity of the earthquakes is appraised by the physical features of the teleseismic source time functions. These features include the overall duration, multiple or single event character, individual source pulse widths, and roughness of the time function. The above measures of source size and complexity can then be compared with the age of subducted lithosphere, plate convergence rate, and other physical parameters of subduction zone [11]. Such comparisons are important for increasing our understanding of the worldwide distribution of the largest earthquakes and their radiated energy. Recent studies of large subduction zone earthquakes suggest that the maximum observed earthquake for a given trench is directly related to the degree of coupling between the plates and the size of fault asperities [28]. Ruff and Kanamori [23] found a significant relationship between the age of the subducting lithosphere, convergence rate, and maximum M_w. Trenches subducting younger crust with higher convergence rates were found in general to produce larger earthquakes. Higher convergence rates and younger, more buoyant crust are thought to cause larger earthquakes by producing strong coupling between the plates. In the asperity model of subduction zone earthquakes, stronger coupling is a direct result of greater areas of the fault plane supporting the accumulated stress between the plates. These

areas rupture relatively coherently during an earthquake and are termed asperities.

The earthquakes larger than about M_s 6.9 can rarely be represented by a single point source, even at the wavelengths recorded by the *WWSSN* 15-100 long period instruments (with a peak response at about 15*s* period). These earthquakes usually consist of several discrete ruptures, separated by several seconds in time and several *km* in space, often occurring on faults with different orientations [4]. This is believed to be an expression of fault complexity and the heterogeneity of the faulting process at the earthquake source. Two models have been proposed to explain this heterogeneity; the barrier model [6] and the asperity model [16].

4. Interpretation and Discussion

1 September 1962 earthquake (No. 1).

Source time function (*STF*) shows different time characteristics of energy release, see Figure (3). The 1962 September 1 Buyin Zahra earthquake (M_S 7.2, m_b 6.9) devastated the area south of Qazvin in northern Iran, killing around 12200 people [1]. A displacement generally implies an oblique faulting involved both thrusting on planes dipping south and also left-lateral strike-slip. Average amplitudes were about 1.4*m* vertical displacement and 0.6*m* strike slip [22]. The natures of source time function complexity of two-subevent show that the most part of the seismic moment release in rise (stress increase) and fall (stress decrease) time portion. However we can see the source time function has about 7-second flat duration between two subevent which is related to the lowest stress accumulation in this segment. The rise time of the subevent 1 (τ_r ~ 4.6) is greater than subevent 2 (τ_r ~ 2.5) and pulse duration of both subevents are approximately to equal. The slow rise time presumably results from a very low stress drop. The small slip (40° of this event indicates that asperities are not apparently regions of high strength. Because the concentration of slip on asperities implies that they are regions of high moment release. This implies that a fundamental difference in the fault behavior at the asperity compared with that of the surrounding this fault can occur.

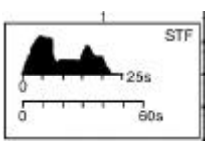

Figure 3. Far-field source time function of the 1962 Buyin Zahra earthquake showing emergent seismic moment release [22].

Figure (4) shows the far-field source time function of the following earthquakes.

3 January 1969 (No. 2), 30 July 1970 (No. 3), 22 February 1984 (No. 11), 6 March 1986 (No. 13), 14 February 1971 (No. 4), 17 September 1989 (No. 16), 28 November 1991 (No. 18) earthquakes.

These earthquakes have large moment release in the first part of the process, while ratios of subevents for foreshock of events numbers 13 and 18 occurs in the last part and initiate small release followed after 4*s* and 2s by a larger one respectively, see Figure (4). Events 3, 11, and 16 show a complex rupture process formed more than 2 subevents. In conjunction with the spatial and temporal behavior of these events the complexity of rupture suggests that strain accumulated gradually in a system of faults in the sediments, granite and basaltic region [22]. The effect of a critical rupture (the first event of the main shock) was to cause a rapid release of stress (dominant event of the main shock) as well as a more gradual release of stress (the other subevents) on adjacent coplanar and conjugate faults.

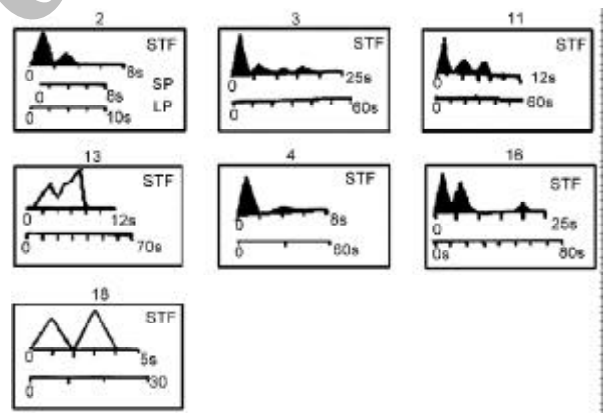

Figure 4. Far-field source time functions of the 3 January 1969, 30 July 1970, 22 February 1984, 6 March 1986, 14 February 1971, 17 September 1989, 28 November 1991 earthquakes showing emergent seismic moment release [15, 22].

Figure (5) shows the far-field source time function of the following earthquakes.

4 November 1978 (No. 5), 19 December 1980 (No. 7), 7 September 1987 (No. 14), 16 September 1989 (No. 15), 4 May 1980 (No. 6), 31 August 1993 (No. 19), 1 July 1994 (No. 20), 29 October 1995 (No. 22), 4 February 1997 (No. 24) 28 February 1997 (No. 25), 9 July 1998 (No. 26), 22 August 2000 (No. 27), 25 November 2000 (No. 28), 6 December 2000 (No. 30) earthquakes.

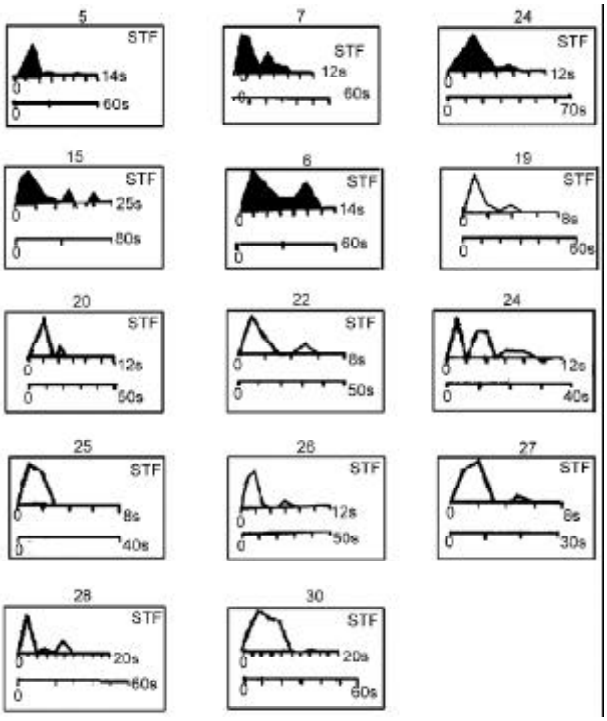

Figure 5. Far-field source time functions of the 4 November 1978, 19 December 1980, 7 September 1987, 16 September 1989, 4 May 1980, 31 August 1993, 1 July 1994, 29 October 1995, 4 February 1997, 28 February 1997, 9 July 1998, 22 August 2000, 25 November 2000, 6 December 2000 earthquakes showing emergent seismic moment release [15, 22].

All *STF* (except event 24) start with a high release of energy in first part of the first subevent. Varying the seismic moment along total duration of *STF* is directly related to varying the source velocity structure which did have an effect on centroid depth and seismic moment. In addition uncertainties in attenuation factor, t^*, mainly affect estimates of source duration and seismic moment. The *STF* of these events show that the rupture characteristics contain a different size of subevents with same shape and same rupture history. The rise time of subevent 1 is larger than another subevents and most part of seismic moment releases in first rupturing process. The nature of this function show that the faulting consists of several fractures separated by strong barriers, which remain unbroken after the event. If the barriers are completely broken, there may be no aftershocks within the main-shock fault plane. The emergent nature of the seismic moment release observed in the rise time of the source time function suggests no difficulties in breaking the barriers. Earthquake with larger magnitude ($M_w \geq 6$) show long duration and complex *STF* (events 15, 24, 25, 28, 30). Events 15 and 24 show a complex rupture process formed by a 3 subevents with a shorter *STF* for the first one and near to equal duration for event 28. The complexity of the source time function as evidenced by the complexity of the body phases, low fault rupture velocity, is explained in terms of a multiple source.

Figure (6) shows the far-field source time function of the following earthquakes.

29 October 1985 (No. 12), 22 December 1980 (No. 8), 4 August 1981 (No. 9), 22 July 1983 (No. 10), 21 June 1990 (No. 17), 1 July 1994 (No. 21), 4 February 1997 (No. 23), 25 November 2000 (No. 29), 10 June 2001 (No. 31) earthquakes.

Events 12, 8, 9, 23 have larger moment release in the first part of the process and consist of several impulses that can be interpreted as a more complex rupture process. Shallow earthquakes 10, 17, 21, 29, and 31 with M_w and epicenter inside the continent show simple *STF*, in general corresponding to a simple impulse of triangular form with short time duration, less than 5s. These shocks can be associated with single ruptures.

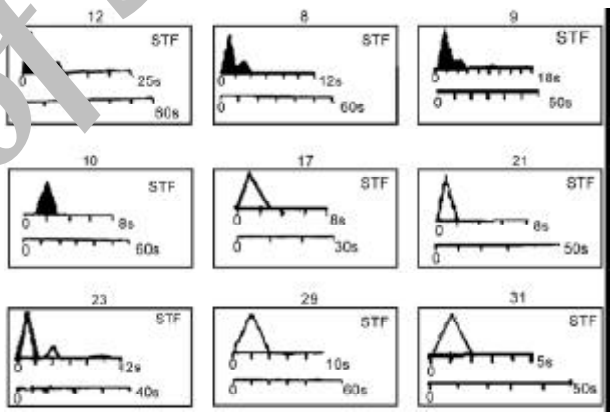

Figure 6. Far-field source time functions of the 29 October 1985, 22 December 1980, 4 August 1981, 22 July 1983, 21 June 1990, 1 July 1994, 4 February 1997, 25 November 2000 earthquakes showing emergent seismic moment release [15, 22].

5. Source Duration versus Seismic Moment and Depth

Table (2) lists the source time parameters determined in this study. Figure (7) shows the measured durations plotted the corresponding moment of total duration. The entire data set is fit by $log\tau_t = 0.2642\ logM_O - 8.9119$. It is expected that in order to obtain moment-duration, the values should lie between $log\tau \propto 0.25\ logM_O$ and $log\tau \propto 1.0\ logM_O$ for shallow earthquakes [7, 8, 9, 16]. As expected, events with large moments tend to have longer durations than events with smaller moments. In addition, the total duration of earthquakes that are used in this study is plotted versus depth, see Figure (8). However, a slight decrease in duration versus

Table 2. Source parameters of largest subevents that is observed from source time functions.

No	Date	f_o (hz)	r_0 (km)	τ_t (sec)	τ_p (sec)	Stress drop (bar)	Displacement (m)
1	01 09 1962	0.0389	33.50	22	8.18	4.279192	3.35
2	03 01 1969	0.0795	16.39	4	2.00	0.1875977	1.639
3	30 07 1970	0.0757	17.22	20	4.20	3.676292	1.722
4	14 02 1971	0.1591	8.20	6	2.00	3.222036	0.82
5	04 11 1978	0.0707	18.43	12	4.50	1.327802	1.843
6	04 05 1980	0.0578	22.5	12	5.50	1.533467	2.25
7	19 12 1980	0.0805	16.20	8.3	3.95	1.442715	1.62
8	22 12 1980	0.1632	7.98	4	1.95	2.412858	0.798
9	04 08 1981	0.1061	12.28	12	3.00	0.5615496	1.228
10	22 07 1983	0.1591	8.192	2	2.00	1.495661	0.8192
11	22 02 1984	0.1632	7.98	8	1.95	4.379209	0.798
12	29 10 1985	0.0848	15.37	10	3.75	2.626085	1.537
13	06 03 1986	0.0795	16.39	7	4.00	2.416934	1.639
14	07 09 1987	0.0539	24.18	8.9	5.90	7.207542	2.418
15	16 09 1989	0.0392	33.52	22.5	8.12	0.81[illegible]9155	3.352
16	17 09 1989	0.0795	16.39	22.5	4.00	2.1[illegible]	1.639
17	21 06 1990	0.1061	12.28	4.2	3.00	0.68660[illegible]	1.228
18	28 11 1991	0.1591	8.19	4	2.00	[illegible]746	0.819
19	31 08 1993	0.1061	12.28	4.85	3.00	0.1493[illegible]33	1.228
20	01 07 1994	0.1196	10.89	5	[illegible]56	0.[illegible]02081	1.089
21	01 07 1994	0.1591	8.19	2	2.[illegible]	0.4733609	0.819
22	29 10 1995	0.1068	12.20	6	[illegible]98	0.293588	1.22
23	04 02 1997	0.1591	8.192	10.95	2.0[illegible]	1.280859	0.8192
24	04 02 1997	0.1591	8.192	11	[illegible]0	45.74496	0.8192
25	28 02 1997	0.0994	13.11	[illegible]	3.20	2.32812	1.311
26	09 07 1998	0.0936	13.92	[illegible]7	3.40	0.709523	1.392
27	22 08 2000	0.1061	12.28	[illegible]3	3.00	0.7290708	1.228
28	25 11 2001	0.0795	16.3[illegible]	12	4.00	2.322638	1.6395
29	25 11 2000	0.0795	[illegible]395	4	4.00	1.65761	1.6395
30	06 12 2000	[illegible]06[illegible]36	19.[illegible]04	10	5.00	12.24766	1.964
31	10 06 2001	0.1[illegible]1	[illegible].192	4	2.00	0.9363795	1.964

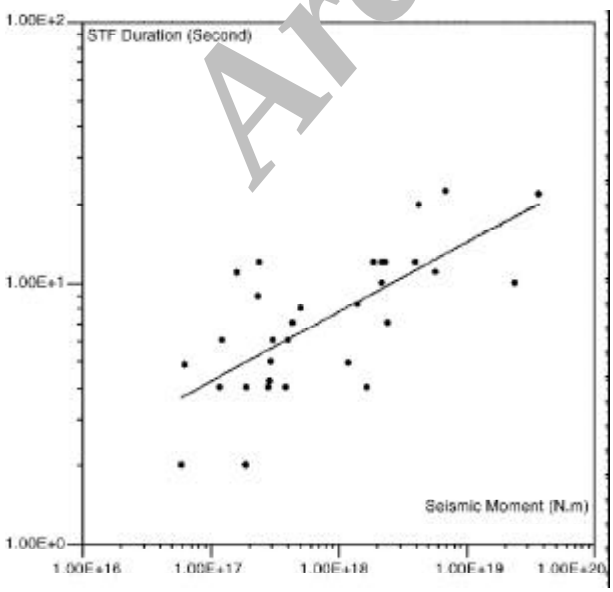

Figure 7. Source duration (τ_t) versus seismic moment (M_O).

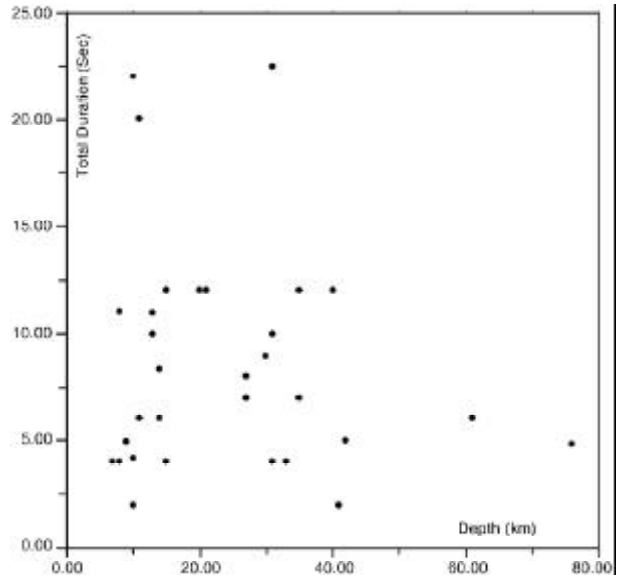

Figure 8. Total durations as listed in Table (2) plotted versus depth.

depth result for deep earthquakes [5] has not been found for shallow events that are used in this study. This maybe results due to the non-homogeneity of material strength along the plane of rupture in crustal earthquakes. Table (3) shows the result of regression, $\log \tau_t = c \log M_O + d$ for different tectonic regions.

Table 3. Result of regression for different tectonic regions.

Region	Total Duration (τ_t)	Reference
Caspian Sea and Surrounding Area	C = 0.264 ± 0.0001 d = -8.911± 0.194	This study
Mexico	C = 0.363 ± 0.014 d = -8.619 ± 0.337	Singh et al, 2000
Mexico and Kanto	C = 0.365 ± 0.011 d =- 8.706 ± 0.262	Singh et al, 2000
Mexico, Kanto, California, and Deep	C = 0.363 ± 0.008 d = -8.580 ± 0.190	Singh et al, 2000

Comparison of *c* parameter between the above different tectonic regions shows that the Caspian sea and the surrounding area has the lowest slop than the other regions. The seismicity in Caspian sea and surrounding area has continental intraplate characteristics. But the seismic activities in Mexico Kanto and California regions have oceanic interplate features [24]. The comparison of homogeneity between both different tectonic regions shows that this parameter in oceanic plate is more than continental plates. In addition, the seismic signal in this area (oceanic interplate) is less attenuative than other continental intraplate regions. In this region, the body wave phases with longer duration can be observed in oceanic intraplate regions than continental intraplate area. It can be clearly seen that the slop value in oceanic plate is greater than Caspian and surrounding area.

The corner frequency is approximately given by $f_0 = 1/\pi\tau_p$ where τ_p is the largest pulse duration [13, 14]. The essential purpose of calculates corner frequency is to evaluate the source dimension. Then the source radius using Brune [2] relation for a circular fault is calculated using 3.5*km/s*, see Table (2) for rupture velocity.

$$R = 2.34v/2\pi f_0 \quad (1)$$

For event 13, the *S* wave spectrum from seismograms recorded at Ashghabad [10] and *s* coda spectrum are complex, showing a constant low frequency level at 0.08*Hz* (The result of present study show that the corner frequency is 0.079*Hz*, Table (2)).

The mean stress drop (Ds) is calculated by using the mean moment and mean radius [2]:

$$\Delta\sigma = 7M_0 / 16R^3 \quad (2)$$

The moment values obtained from inversion technique [15, 22] have been used for calculated of the stress drop at this study. Lines of constant stress drop appropriate for the Savage [25] model described are drawn on the log moment-log frequency plot, see Figure (9).

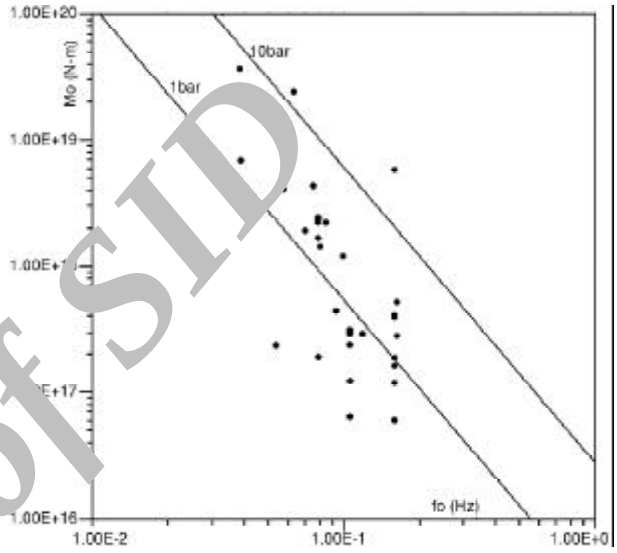

Figure 9. The relationship between M_O and f_o obtained in the present study.

In the case of the corner frequency f_0 listed in Table (2), there does not appear to be a systematic difference between the values estimated for the same earthquake. Following Hanks and Thatcher [12], we have plotted M_O as a function of f_0 in Figure (9) for events reported in Table (2). It is found that f_0 slightly increases with decreasing M_O. The present data do not allow any strong conclusions to be drawn concerning the existence of a systematic relation between f_0 and M_O.

Stress drops range from just less than one to few tens of bar, see Figures (9) and (10) and Table (2). The stress drop values are plotted in Figure (10) to document any possible dependence on depth. Particularly for normal faulting, the weight of the overburden would tend to increase with depth, although a regional stress field may exist that would cancel the effect of the weight of the overburden.

The seismic moment, M_O, is given by $M_O = \mu Au$ where μ is the rigidity ($\sim 3\times 10^{10} Nm^{-2}$), A is the fault

area, and u is the average displacement. Let us assume that the fault is roughly circular in area with diameter L, and the ratio u/L is $\sim 5\times 10^{-5}$ [27]. The displacement value for each event is observed and the displacement contour map for the study area is prepared, see Table (2) and Figure (11).

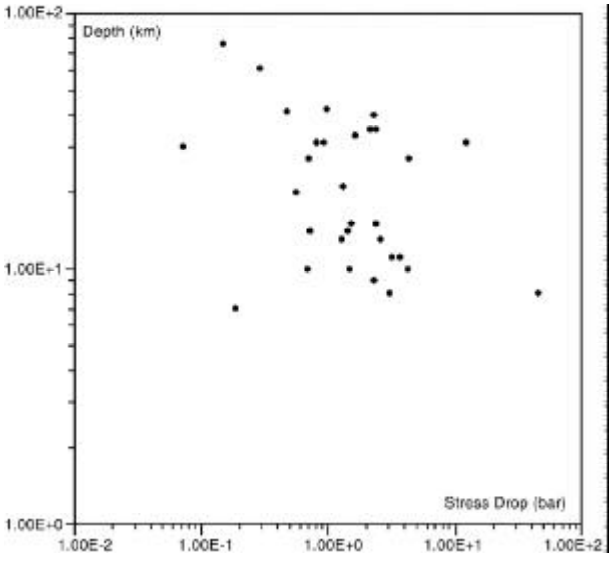

Figure 10. The relationship between depth and stress drop obtained in the present study.

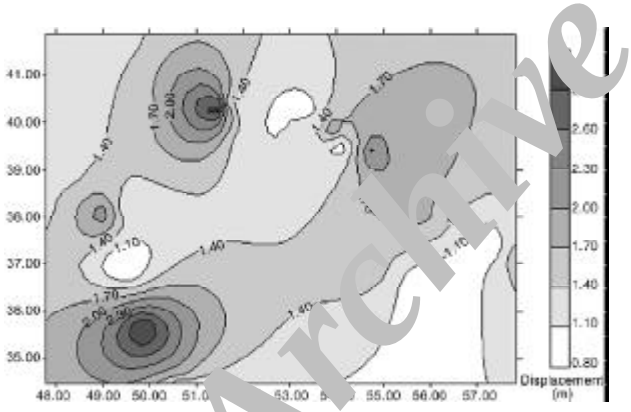

Figure 11. Displacement contour map prepared for Caspian sea and surrounding area.

6. Conclusions

In this study source characteristics detectable from source time function investigate to examine a possible depth dependence in source properties for crustal earthquakes. No clear depth dependence with source duration was found. The source time function of these earthquakes show that the faulting in the Caspian region consists of several fractures separated by strong barriers, which remain unbroken after the event. If the barriers are completely broken, there may be no aftershocks within the main shock fault plane. Source time functions show different characteristics depending on the magnitude and depth of the earthquakes. Shallow earthquakes located offshore with large magnitude show complex *STF* and long time duration. Within the continent, shallow earthquakes show less complexity and *STF* have shorter duration. The major conclusion of this paper is illustrated in Figures (7), (8) and (9): the uncertainties in the determination of pulse width and seismic moment, does not appear to be significant. Errors in the pulse width arise from scattering of the wave. In addition, some variation in pulse width between stations for a given event could be caused by source directivity. Without sufficient azimuthal coverage, however, the rupture geometry cannot be constrained well enough to correct the pulse widths. Additional error in the stress drop determination is produced by uncertainty in the seismic moment. Scatter in the seismic moment values is caused by the site conditions and errors in the radiation pattern corrections. The stress drop of an earthquake must represent the minimum tectonic stress operative to cause the event, as well as a minimum estimate of material strength near the rupture surface. The proximity of low and high stress drop events indicates inhomogeneities in stress or material properties within a rupture zone.

Acknowledgments

The authors have benefited greatly from the review of three anonymous reviewers. This work has been supported by *IIEES*, project *ZLM*-16/767.

References

1. Ambraseys, N. N. (1963). "The Buyin Zahra (Iran) Earthquake of September 1962: A Field Report", *Bull. Soc. Am.*, **53**, 705-740.

2. Brune, J.N. (1970). "Tectonic Stress and the Spectra of Seismic Shear Waves from Earthquakes", *J. Geophys. Res.*, **75**, 4997-5009.

3. Brune, J.N. (1971). "Tectonic Stress and the Spectra of Seismic Shear Waves from Earth quakes: Correction", *J. Geophys. Res*, **76**, p. 5002.

4. Butler, R., Stewart, G.S., and Kanamori, H. (1979). "The July 27 1976 Tangshan China Earthquake - A Complex Sequence of Intraplate Events", *Bull. Seism. Soc. Am.*, **69**, 207-220.

5. Bos, A.G., Nolet., G., Rubin, A., Houston, H., and Vidale, J.E. (1998). "Duration of Deep Earthquakes Determined by Stacking of Global Seismograph Network Seismograms, *J. Geophys. Res.*, **103**(B9), 21059-21065.

6. Das, S. and Aki, K. (1977). "Fault Plane with Barriers: A Versatile Earthquake Model", *J. Geophys. Res.*, **82**, 5658-5670.

7. Ekstom, G. and Engahl, R. (1989). "Earthquake Source Parameters and Stress Distribution in the Adak Island Region of the Central Aleutians Islands", *J. Geophys. Res.*, **94**, 15499-15519.

8. Ekstom, G., Stein, R.S., Eaton, J.P., and Eberhart-Phillips, D. (1992). "Seismicity and Geometry of a 100-km Long Blind Thrust 1', The 1985 Ketleman Hills, California Earthquake", *J. Geophys. Res.*, **97**, 4843-4863.

9. Furumoto, M. and Nakanishi, I. (1983). "Source Time Scaling Relation of Large Earthquakes", *J. Geophys. Res.*, **88**, 2191-2198.

10. Golensky, G.L., Kondorskya, N.V., Zakarova, A., Vandeshiva, E., Garagozov, D., Kuliev, F.T., Logova, N.A., Muragov, C.M., Rautian, T.G., Pnake, B.M., Rakemov, A.R ., Rogozhen, E.A., Shavadaiv, R.H., and Chepkunac, L.C. (1989). "The Caspian Earthquake of March 6, Earthquakes in the U.S.S.R. in 1986", Academii Nauk SSSR, 58.

11. Hartzell, S. and Heaton, T. (1985). "Teleseismic Time Functions for Large, Shallow Subduction Zone Earthquakes", *Bull. Seism. Soc. Am.*, **75**(4), 965-1004.

12. Hanks, T.C. and Thatcher, W. (1972). "A Graphical Representation of Seismic Source Parameters", *J. Geophys. Res.*, **77**, 4393-4405.

13. Husebye, E.S. and Mykkeltveit, S. (1980). "Identification of Seismic Sources Earthquake or Underground Explosion", *Proceeding of the NATO Advanced Study Institute Held at Voksenasen*, Oslo, Norway, 72-97.

14. Helmberger, D.V. and Malone, S.D. (1975). "Modeling Local Earthquakes as Shear Dislocations in a Layered Half-Space", *J. Geophys. Res.*, **80**, 4881-4888.

15. Jackson, J., Priestly, K., Allen, M., and Berberian, M. (2002). "Active Tectonics of the South Caspian Basin", *Geophys. J. Int.*, **148**, 214-245.

16. Kanamori, H. and Giwen, J.W. (1981). "Use of Long Period Surface Waves for Rapid Estimation of Earthquake Source Parameters", *Phys. Earth Planet*, Interiors 27, 8-31.

17. Kikuchi, M. and Ishida, M. (1993). "Source Retrieval for Deep Local Earthquakes with Broad Band Records", *Bull. Seism. Am.*, **83**, 1855-1870.

18. Kanamori, H. and Stewart, G.S. (1978). "Seismological Aspects of the Guatemala Earthquake", *J. Geophys. Res.*, **83**, 3427-3434.

19. McCaffery, R. and Abers, G. (1988). "Syn3: A Program for Inversion of Teleseismic Body Wave Forms on Microcomputers", Air Force Geophysics Laboratory Technical Report, AFGL-TR-88-0099, Hanscomb Air Force Base, MA.

20. McCaffery, R., Abers, G., and Zwick P. (1991). "Inversion of Teleseismic Body Waves", In: Digital Seismogram Analysis and Waveform Inversion (ed. By W.H.K. Lee), IASPEI Software Library, **3**, 81-166.

21. Nabelek, J.L. (1984). "Determination of Earthquake Source Parameters from Inversion of Body Waves", Ph.D. Thesis, MIT, Cambridge, MA.

22. Priestly, K., Baker, C., and Jackson, J. (1994). "Implication of Earthquake Focal Mechanism Data for the Active Tectonics of the South Caspian Basin and Surrounding Regions", *Geophys. J. Int.*, **118**, 111-141.

23. Ruff, L. and Kanamori, H. (1980). "Seismicity and the Subduction Process", *Phys. Earth Planet,* Interiors, **23**, 240-252.

24. Singh, K., Pacheco, J., Ordaz, M., and Kostoglodov, V. (2000). "Source Time Function and Duration of Mexican Earthquakes", *Bull. Seism. Soc. Am.*, **90**(2), 468-482.

25. Savage, J.C. (1972). "The Relation of Corner Frequency to Fault Dimensions", *J. Geophys. Res.*, **77**, 3788-3795.

26. Wyss, M. and Brune, J.N. (1971). "Regional Variations of Source Properties in Southern California Estimated from the Ratio of Short to Long Period Amplitudes", *Bull. Seism. Soc. Am.* **61**, 1153-1168.

27. Scholtz, C.H., Aviles, C.A. and Wessnousky. S.G. (1986). "Scaling Differences Between Large Interplate and Intraplate Earthquakes", *Bull. Seism. Soc. Am.*, **76**, 65-70.

28. Uyeda, S. and Kanamori, H. (1983). "Bac-Arec Opening and the Mode of the Subducting", *J. Geophys. Res.*, **84**, 1049-1061.